Focal volume optics for composite structuring in transparent solids

Zhang, B.; Wang, Z.; Tan, D.Z.; Gu, M.; Yue, Yuanzheng; Qiu, J.R.

Published in:
International Journal of Extreme Manufacturing

DOI (link to publication from Publisher):
10.1088/2631-7990/ad8712

Publication date:
2025

Document Version
Publisher's PDF, also known as Version of record

Focal volume optics for composite structuring in transparent solids

OPEN ACCESS
IOP Publishing | IMMT
International Journal of Extreme Manufacturing
Int. J. Extrem. Manuf. 7 (2025) 015002 (10pp)
https://doi.org/10.1088/2631-7990/ad8712

Focal volume optics for composite structuring in transparent solids

Bo Zhang[1,7], Zhuo Wang[1,7], Dezhi Tan[2,3,*], Min Gu[4,5], Yuanzheng Yue[6] and Jianrong Qiu[1,*]

[1] State Key Laboratory of Modern Optical Instrumentation, College of Optical Science and Engineering, Zhejiang University, Hangzhou 310027, People's Republic of China
[2] Zhejiang Lab, Hangzhou 311100, People's Republic of China
[3] School of Materials Science and Engineering, Zhejiang University, Hangzhou 310027, People's Republic of China
[4] Institute of Photonic Chips, University of Shanghai for Science and Technology, Shanghai, People's Republic of China
[5] Centre for Artificial-Intelligence Nanophotonics, School of Optical-Electrical and Computer Engineering, University of Shanghai for Science and Technology, Shanghai, People's Republic of China
[6] Department of Chemistry and Bioscience, Aalborg University, 9220 Aalborg, Denmark

E-mail: wctdz@zju.edu.cn and qjr@zju.edu.cn

Received 12 March 2024, revised 17 June 2024
Accepted for publication 15 October 2024
Published 5 November 2024

Abstract

Achieving high-level integration of composite micro-nano structures with different structural characteristics through a minimalist and universal process has long been the goal pursued by advanced manufacturing research but is rarely explored due to the absence of instructive mechanisms. Here, we revealed a controllable ultrafast laser-induced focal volume light field and experimentally succeeded in highly efficient one-step composite structuring in multiple transparent solids. A pair of spatially coupled twin periodic structures reflecting light distribution in the focal volume are simultaneously created and independently tuned by engineering ultrafast laser-matter interaction. We demonstrated that the generated composite micro-nano structures are applicable to multi-dimensional information integration, nonlinear diffractive elements, and multi-functional optical modulation. This work presents the experimental verification of highly universal all-optical fabrication of composite micro-nano structures with independent controllability in multiple degrees of freedom, expands the current cognition of ultrafast laser-based material modification in transparent solids, and establishes a new scientific aspect of strong-field optics, namely, focal volume optics for composite structuring transparent solids.

Supplementary material for this article is available online

Keywords: ultrafast laser, focal volume light field, composite structuring, transparent solids, advanced manufacturing

[7] These authors contributed equally to this work.
[*] Authors to whom any correspondence should be addressed.

2631-7990/25/015002+10$33.00

1. Introduction

Micro-nano structures lay at the heart of optical components for light manipulation in different dimensions [1–6]. In particular, composite micro-nano structures constructed in 3D have been revealed to enable novel photonic devices with unprecedented control degrees of freedom over the state of electromagnetic waves and have emerged as a new research frontier in nanophotonic science and engineering [7–10]. For example, multi-layer composite micro-nano structures allow for modulating light waves that have wave vectors in 3D space, enabling innovation in stereoscopic display, light manipulation, and data storage [11–15]. Currently, the generation of composite micro-nano structures largely relies on complicated multi-step micro-nano machining processes where the integration of different structural characteristics remains limited. Fast construction of composite micro-nano structures with a higher level of integration in 3D space has long been a bottleneck due to the lack of effective fabrication approaches.

Ultrafast laser-matter interaction has become an excellent platform for preparing functional elements in transparent media [16–22]. For example, ultrafast laser-induced embedded micro-nano structures have been widely studied and utilized in the welding of all-inorganic hard and brittle transparent materials [23, 24]. In particular, 3D material modification capability has become one of the most important attributes inherent in ultrafast laser direct writing (ULDW) technology [25–29]. However, creating different types of micro-nano structures in one step with a single-beam ultrafast laser is traditionally very difficult and even generally not within the scope of ULDW, which is essentially restricted by assuming the typical light distribution as the Gaussian type in the focal volume. Generally, achieving composite structuring with multiple degrees of freedom requires a higher-level manipulation of micro-scale spatial light fields. Up to now, it remains a great challenge to determine and control the microscopic optical behaviors of highly intense light-matter interaction in the focal volume at the micro-nano scale, owing to the multiple complex optical responses and fast ionization process [30–33].

Here, we realize the generation, visualization, and manipulation of the focal volume light fields induced during the ultrafast laser-matter interaction. Combined with ULDW, we proposed that such light fields can be applied for highly integrated and controllable single-step composite structuring within the focus of a single-beam ultrafast laser. Our principles are confirmed to be highly universal and widely applicable in different types of transparent dielectrics. Finally, multiple applications are demonstrated using the fabricated composite structures.

2. Results and discussion

2.1. Working principle of composite structuring

In ultrafast laser-matter interaction, a tightly focused ultrafast laser can induce multi-photon ionization in various transparent dielectrics. This process is highly dependent on the intensity of the laser beam and thus occurs exclusively within the focal volume [34, 35]. During multi-photon ionization, a significant number of free electrons can be quickly excited (figure S2 in the supplementary material), causing the ionized material within the focal volume to exhibit a quasi-metallic state with metal-like optoelectronic properties [36, 37]. Such an ionized zone will disturb the subsequent incident light wave. Here, we proposed that the ionized zone can serve as a tunable scatterer to the incident light and lead to the generation of a tunable scattering light field in the focal volume (figure 1(a)). Generally, a smaller and rounder scatterer leads to an intense forward light field, while a larger and longer scatter leads to a sideward light field in the focal volume (figures S3 and S4 in the supplementary material). The interference between the incident light and the scattered light occurs in the focal volume, resulting in an intense 3D volumetric light field (figures 1(b)–(i)). Both the well-defined intensity distribution and the extremely confined interaction scope make this volumetric light field an ideal secondary driving source to trigger structured spatial nonlinear absorption and selectively modify local material, thereby producing wavelength-scaled periodic interference patterns (PIPs) with a period of $\sim$1 μm (figure 1(b)–(ii)). During the generation process of PIPs, nano-plasmas could be simultaneously excited by ultrafast laser irradiation and their anisotropic growth induced by local field enhancement leads to nano-scale periodic material modification within the volumetric light field-irradiated area, whose orientation depends on the light polarization [38–40]. Therefore, this well-structured volumetric light field can be adopted to further induce subwavelength-scaled nano-gratings (NGs) with a period of $\sim$200 nm, which are embedded inside the PIPs (figure 1(b)–(iii)). This process allows for two parallel material modifications within the extremely compact space of a laser focus and constructing two different yet coupled periodic structures at the same 3D spatial location, namely, single-step composite structuring (figure 1(b)). As a result, we established a fundamentally new principle to achieve highly integrated composite structures relying on the intrinsic light field distribution in the focal volume based on the ultrafast laser-matter interaction.

2.2. Manipulation of composite structuring

Although the PIPs and NGs are spatially coupled together, forming composite structures, they can be manipulated continually and independently (figures 2(a) and (d)), as the orientation of PIPs and NGs depends on the laser scanning direction and polarization, respectively, which is due to the different physical origins (figure S5 and equations (S2)–(S6) in the supplementary material). We identified the formation and orientation of NGs by birefringence intensity mapping (figures 2(b) and (e)) and slow-axis azimuth imaging of the birefringence area (figures 2(c) and (f)), which confirms the optical phase-modulation ability and structural variation of NGs. In addition, we demonstrated that the PIPs and the NGs can be synergistically tuned by simultaneously adjusting the

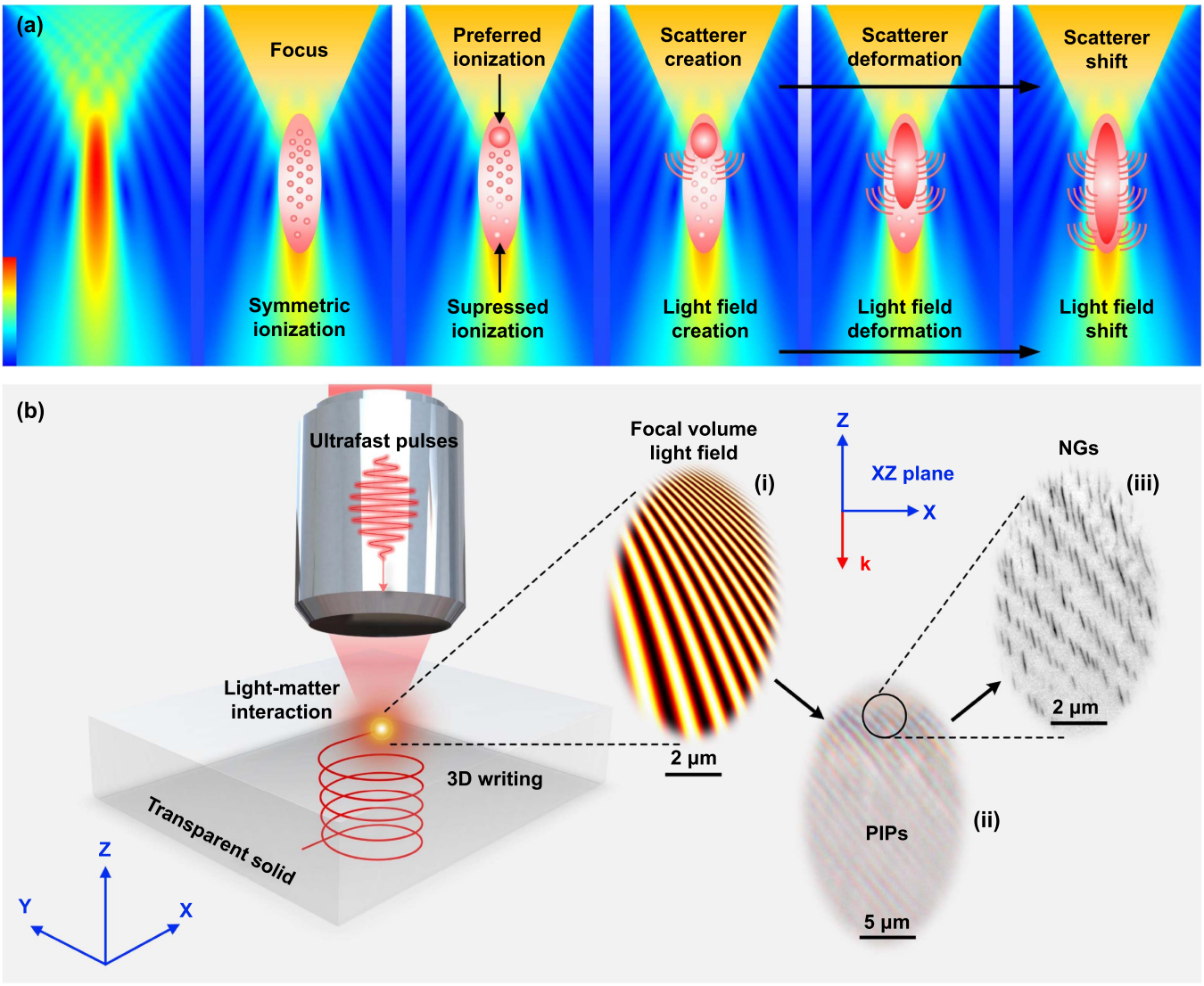

Figure 1. Conceptual model for the principle of composite structuring. (a) Schematic of the light field creation and evolution in the focal volume of a gaussian ultrafast laser beam irradiating in transparent dielectrics. Radiating symbols indicate light scattering. (b) Composite structuring with focal volume light field. Insets: theoretical volume light field in the *XZ* plane (i), experimentally observed periodic interference patterns (PIPs) in the *XZ* plane (ii), and experimentally observed nano-gratings (NGs) inscribed inside the PIPs. (iii) k indicates the laser propagation direction.

scanning direction and laser polarization (figures 2(g) and (i)). Notably, the existence and variation of PIPs do not disturb the birefringence-related optical signals created by NGs, which indicates that both the manipulation and identification of these two structures are completely decoupled. These findings indicate that focal volume light fields enable composite structuring (3D writing, PIPs creation, and NGs creation) with independent controllability in multiple degrees of freedom (3D spatial coordinates, scanning direction, and polarization direction). In contrast to conventional micro-nano machining principles that rely on special materials and multi-step processes to realize the fabrication of different types of micro-nano structures, the composite structuring capacity proposed here is inherent to ultrafast laser processing.

According to our interference model (equations (S2)–(S5)), the spatial distribution of the constructive interference field in the focal volume is theoretically a series of hyperboloids, each of which corresponds to the interference field under a specific interference order. As the focal volume light field is essentially the 3D constructive interference established at the focus, the created PIPs inherit the structural characteristics of the volume light field, which can be verified by their intersecting patterns in the *XZ*, *YZ*, and *XY* planes (figures S6(a)–(c) in the supplementary material). Based on this, the experimentally observed PIPs can be quantitatively described by the projection of these hyperboloids in observation planes, denoted as constructive interference stripes (CISs). For instance, the CISs in the *XY* plane are a series of circular arcs and the CISs in the *YZ* plane

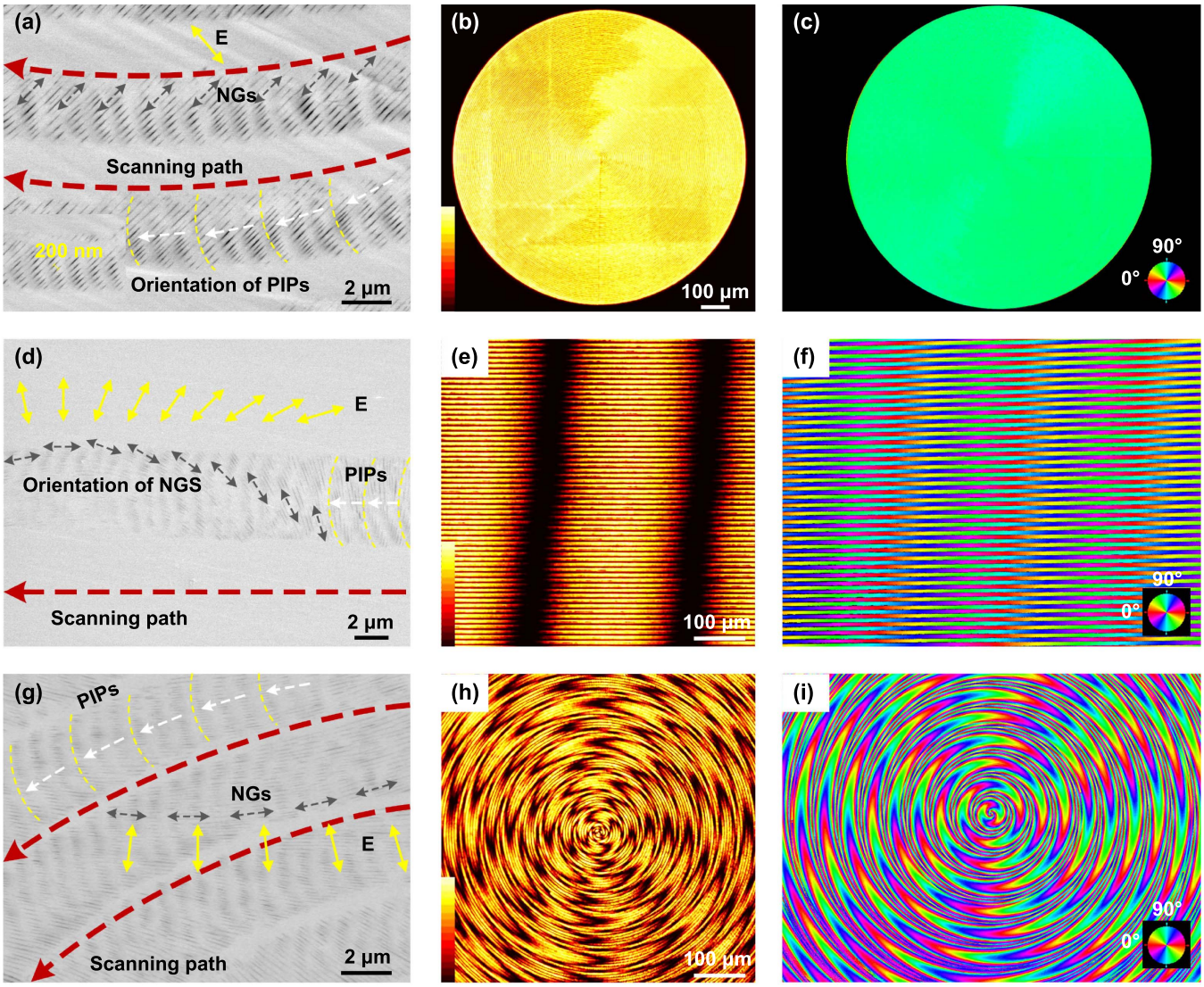

Figure 2. Composite structuring control and corresponding optical characterization in the *XY* plane. (a), (d), and (g) scanning electron microscopy (SEM) images of the composite structures in fused silica. Inset: partially enlarged image. Red dotted arrows indicate the scanning path. White dotted arrows indicate the orientation of the PIPs. Gray dotted arrows indicate the orientation of the NGs. Yellow dotted curves help to visualize the PIPs. E indicates laser polarization. (b), (e), and (h) birefringence imaging, and (c), (f), and (i) imaged azimuth angles of the slow axis of the birefringence area. Color bars illustrate the birefringence intensity. Pseudocolor indicates the orientation of the slow axis. (a), (b), and (c) the scanning direction is continuously changed and the laser polarization is fixed. (d), (e), and (f) the laser polarization is continuously changed and the scanning direction is fixed. (g), (h), and (i) both the laser polarization and the scanning direction are continuously changed.

are a series of symmetrical hyperbolic curves. Notably, the existence of the inclination factor θ (caused by the convergence angle of laser focusing) breaks the symmetry of the CISs in the *XZ* plane (equation (s6)), dividing the CISs into three main categories, namely, positive, negative, and zero-order CISs (figures S6(d)–(f) in the supplementary material). Under the restriction of interference orders, the creation of PIPs must follow specific patterns, which lays the foundation for achieving more complex manipulation of composite structuring.

Here, we propose that this structural manipulation essentially manifests as the shift of CISs that work in composite structuring, which can be demonstrated by examining the PIPs formed in different media. Theoretically, owing to the difference in nonlinear optical response properties between different media, the creation of PIPs should be induced by different types of CISs. Here, we present three representative experimental results of PIPs induced in different media, including positive CISs-induced PIPs in La_2O_3–Nb_2O_5 glass that tilt in the direction opposite to the scanning direction (figure 3(a), left), negative CISs-induced PIPs in La_2O_3–Al_2O_3 glass that tilt along the scanning direction (figure 3(b), left), and zero-order CISs-induced PIPs in fused silica (figure 3(c), left). These experimentally induced PIPs are in good agreement with the simulated CISs in the red-marked regions (figures 3(a)–(c), right).

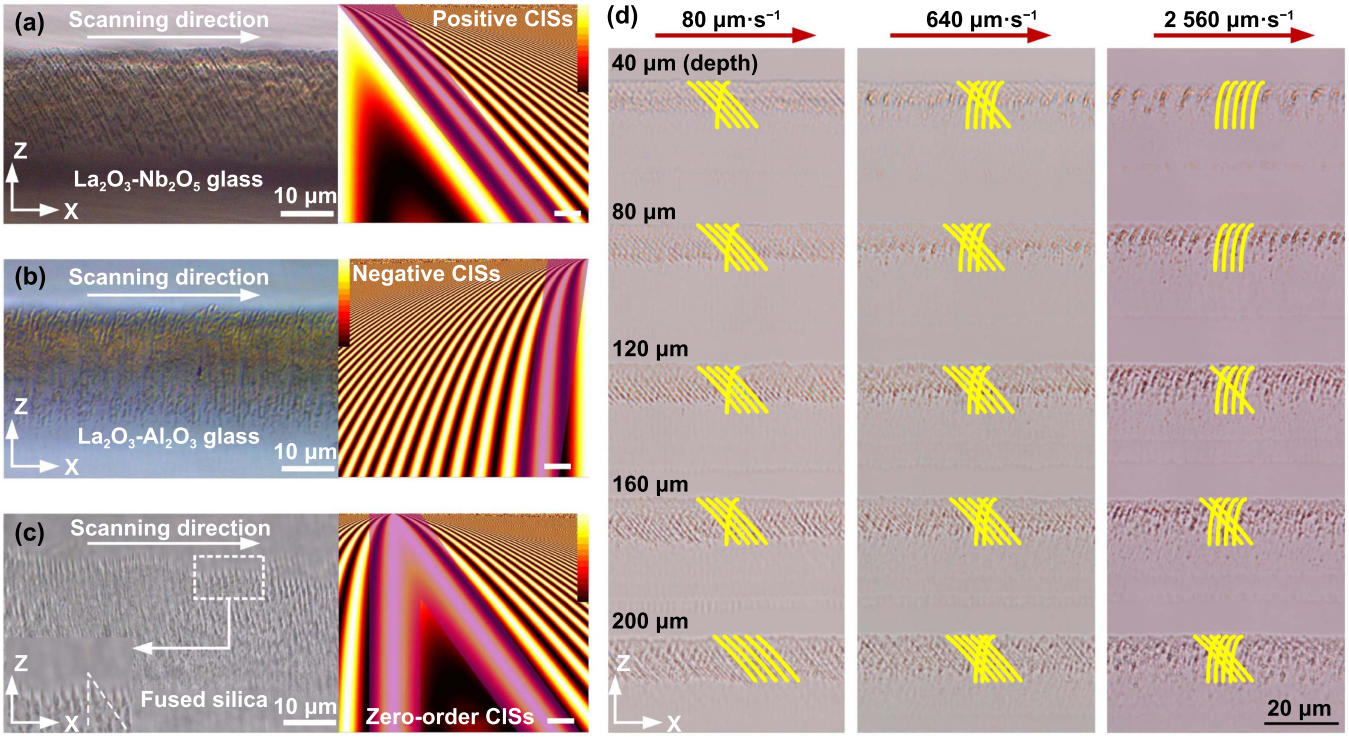

Figure 3. Interference-based composite structuring manipulation. (a) PIPs created in the La_2O_3–Nb_2O_5 glass (left) and simulated positive CISs (right). (b) PIPs created in the La_2O_3–Al_2O_3 glass (left) and simulated negative CISs (right). (c) PIPs created in the fused silica (left) and simulated zero-order constructive interference field (right). The regions marked in red indicate effective CISs that dominate the PIPs formation. Color bars: light intensity. Scale bars in simulation: 1 μm. (d) Parameter-driven structural manipulation of PIPs in fused silica realized by varying laser scanning speed and writing depth. Red arrows: laser scanning direction. Yellow curves help visualize the gradual transition from positive CISs (bottom left) to negative CISs (top right).

Even in the same medium, the CISs that work in the composite structuring can also be effectively controlled by tuning the processing parameters. These parameters generally enable the scatterer deformation by controlling the incident pulse number per unit length or inducing a self-focusing effect, leading to the shift of CISs. From this, more diverse and fine-grained structural manipulation of the composite structures can be realized. For example, by tuning the scanning speed (pulse density), writing depth, and laser power, the inclination direction of PIPs in fused silica can be gradually shifted from opposite to along the laser scanning direction (figures 3(d) and S7 in the supplementary material), indicating the transition from positive CISs to negative CISs. The PIPs can also be manipulated by adjusting the laser polarization state and the numeric aperture of the objective lens (figure S8 in the supplementary material), implying the highly flexible processing capability of composite structuring.

Generally, the processing parameters (high irradiance, large writing depth, pulse number/density, and focal depth) that contribute to the elongation of the focus tend to activate positive CISs-dominated structuring, while the processing parameters (low irradiance, small writing depth, pulse number/density, and focal depth) that restrain the distortion of the focus tend to activate negative CISs-dominated structuring, which agrees with the model we established (section S2) in the supplementary material.

2.3. Universality of composite structuring

We confirmed that composite structuring can serve as a highly universal composite structuring method that enables the creation of composite structures in multiple transparent dielectrics, including but not limited to sapphire, quartz, lithium niobate, lithium tantalite, and silicon carbide (figure S9 in the supplementary material). Notably, the composite structures exhibit designated structural features by utilizing the phase transition properties of target media, resulting in various advanced functional heterostructures that are not achievable with traditional techniques. Generally, the created composite structures can be categorized into four types by characterizing the inner structures and interfaces (figure 4). The first type of PIPs is characterized by alternately arranged glass arrays with and without defects (type I, figures 4(a) and (e)). The type I PIPs are mainly formed in the media that have low crystallization tendency, such as fused silica. An increase in the crystallization tendency of the media leads to the selective crystallization of the original amorphous matrix, thereby producing periodically arranged crystalline structures. The crystallites can be dispersed (type II, figure 4(b)), for example in La_2O_3–ZrO_2–Nb_2O_5 glass, or fully connected (type III, figures 4(c) and (f)), for example in La_2O_3–Ta_2O_5–Nb_2O_5 glass, depending on the crystallization tendency of different glass matrices. Furthermore, similar phase separations can also be induced

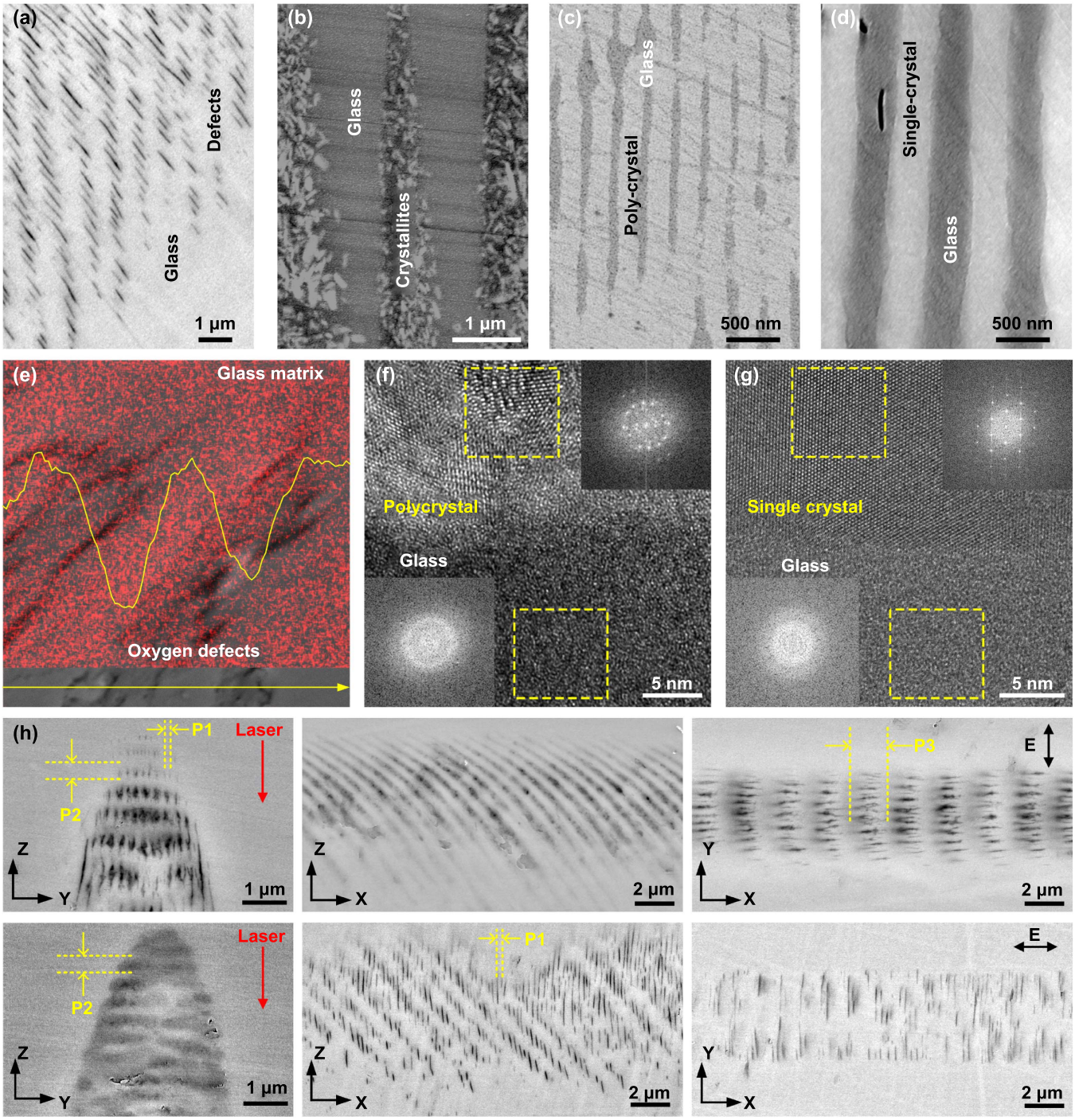

Figure 4. The universality of composite structuring. (a)–(d) SEM images showing the PIPs made of glass-defects (a), glass-crystallites (b), glass-polycrystal (c), and glass-single crystal (d). (e) Mapping of the distribution of O element in the PIPs. The inserted curve indicates O content along the yellow arrow determined by energy dispersive spectroscopy (EDS). (f) High-resolution transmission electron microscopy (HRTEM) image of the heterointerface between glass matrix and polycrystal. (g) HRTEM image of the heterointerface between glass matrix and single crystal. Insets represent the fast Fourier transform (FFT) images of the dotted areas. (h) Cross-section view (right), side view (middle), and top view (left) of the composite structures written with different polarizations. P1, P2, and P3 indicate the periods of PIPs and NGs in different views. E indicates laser polarization direction.

in single crystals (such as quartz and lithium niobate) to produce single crystal-glass PIPs (type IV, figures 4(d) and (g)). Importantly, the structural coupling of PIPs and NGs is also verified to be widely valid in multiple transparent dielectrics, ranging from important glasses to crystals (figure S10 in the supplementary material), and makes the composite structure exhibit multiple periods in 3D space (figure 4(h)), which not only substantiates the universal effectiveness of our principle but also provides a unified mechanism for a series of obscure multi-periodicity phenomena reported before [41–44].

2.4. Potential applications of composite structuring

We presented the potential of the composite structures within multiple aspects of photonics. As the manipulation of PIPs and NGs is completely decoupled, the optical properties of PIPs and NGs can be combined to achieve multi-dimensional information multiplexing. Figures 5(a)–(c) shows that multi-dimensional information integration can be achieved by multiplexing the five dimensions provided by NGs (three spatial dimensions, the azimuth of NGs, and optical retardance) [45, 46], and the sixth dimension, namely the directionality of PIPs, which grants the composite structure with the potential in multi-dimensional information anti-counterfeiting and encryption (figure S11 in the supplementary material). The high universality of composite structuring makes it possible to directly write artificial photonic structures in matrix materials and thus fully utilize the excellent performances of various optical media (figures 5(d) and S12 in the supplementary material), which opens up an avenue to novel optical elements. For example, we demonstrated the fabrication of a planar nonlinear axicon lens with a diameter of about 6 mm in bulk lithium niobate crystal (figure 5(e)). The integration of the nonlinear crystal and the regularly arranged composite structures with sub-wavelength periodicity offers a binary optical manipulation capacity, which allows the element to simultaneously achieve frequency conversion and beam shaping (figure 5(f)). For micro-scale optical modulation, as the period of NGs is sub-wavelength-scaled while that of PIPs is wavelength-scaled, the optical responses of NGs and PIPs can be combined to form a multi-functionally integrated optical modulator that simultaneously possesses polarization and wavelength selectivity (figures 5(g) and (h)).

Compared with the photonic elements that are fabricated by conventional lithography approaches, the created all-inorganic photonic elements embedded in transparent dielectrics generally possess high stability, ultralong service life, and the capacity to work in various extreme environments [47–49]. These photonic elements can potentially be used for the modulation of high-power lasers and effectively work under high temperature, corrosion, and radiation conditions. Predictably, the methodology of focal volume light field-empowered material modification offers an excellent platform for multiple frontier applications, such as optical measurement, information processing, on-chip photonic integration, and space exploration.

3. Discussion and conclusions

For a long time, an ultrafast laser has been applied as a point-typed energy source to trigger various material modifications [50–52], and the profile of light intensity is mainly considered a Gaussian type. Therefore, the actual morphology and evolution of the light field in the focal volume have been overlooked. Our work indicates that the 3D spatial distribution of the light field at the focus can possess finer structures and is tunable, which offers a novel strategy for highly controllable micro-nano fabrication with more degrees of freedom beyond conventional point-by-point optical modification. Furthermore, revealing the actual light field in the focal volume helps understand the ultrafast light-matter interaction physics and may provide the principles for more potential advanced manufacturing technologies.

The proposed models and experimental results may change the traditional cognition of spot-driven laser processing. On the one hand, the focal volume light field can serve as a versatile tool to create various advanced functional composite structures that are not achievable with traditional techniques. On the other hand, the focal volume light field may also become a potentially unfavorable factor in achieving continuous and homogeneous material modification. Therefore, re-examining the current ultrafast laser-based micro-nano manufacturing principle in transparent media would be necessary, and some conventional concepts about behaviors of light in the focal volume need to be improved. This will arouse a series of brand-new research topics about how to activate, manipulate, or eliminate the focal volume light field according to specific application scenarios, which may trigger plenty of research work in the future.

In summary, we proposed and experimentally demonstrated composite material modification in a single step, where the light field in the focal volume can serve as an optical mold for imprinting composite structures and enabling the visualization of the actual energy distribution. The ultrafast laser-excited focal volume light field in transparent dielectrics is revealed to possess a fine distribution rather than being a Gaussian type. The fabricated composite structures are shown to hold great potential for multiple applications, such as multi-dimensional anti-counterfeit, information encryption, nonlinear planar lenses, and multi-functionally integrated photonic crystals. It would be exciting to combine our approach with spatial light modulation technologies, novel photoelectric materials, and intelligent path planning methods to develop a highly generalized strategy to achieve functional photonic elements at the on-demand position in various transparent dielectrics, empowering the construction of next-generation all-inorganic integrated optical systems.

4. Material and methods

4.1. Material preparing

In this study, the unconventional glasses, including La_2O_3–Nb_2O_5 glass, La_2O_3–Al_2O_3 glass, La_2O_3–Ta_2O_5–Nb_2O_5 glass, and La_2O_3–ZrO_2–Nb_2O_5 are prepared using a containerless process where two CO_2 lasers were used to melt the mixture of raw materials levitated by the O_2 airflow. The silica glass and all of the crystals used in this study are commercially available materials.

4.2. Ultrafast laser processing

A ULDW system is used to achieve composite structuring (figure S1 in the supplementary material), where a mode-locked regeneratively amplified Yb: KGW-based ultrafast laser system (PHAROS, Light Conversion Ltd) operating at a wavelength of 1 030 nm was employed as the light source.

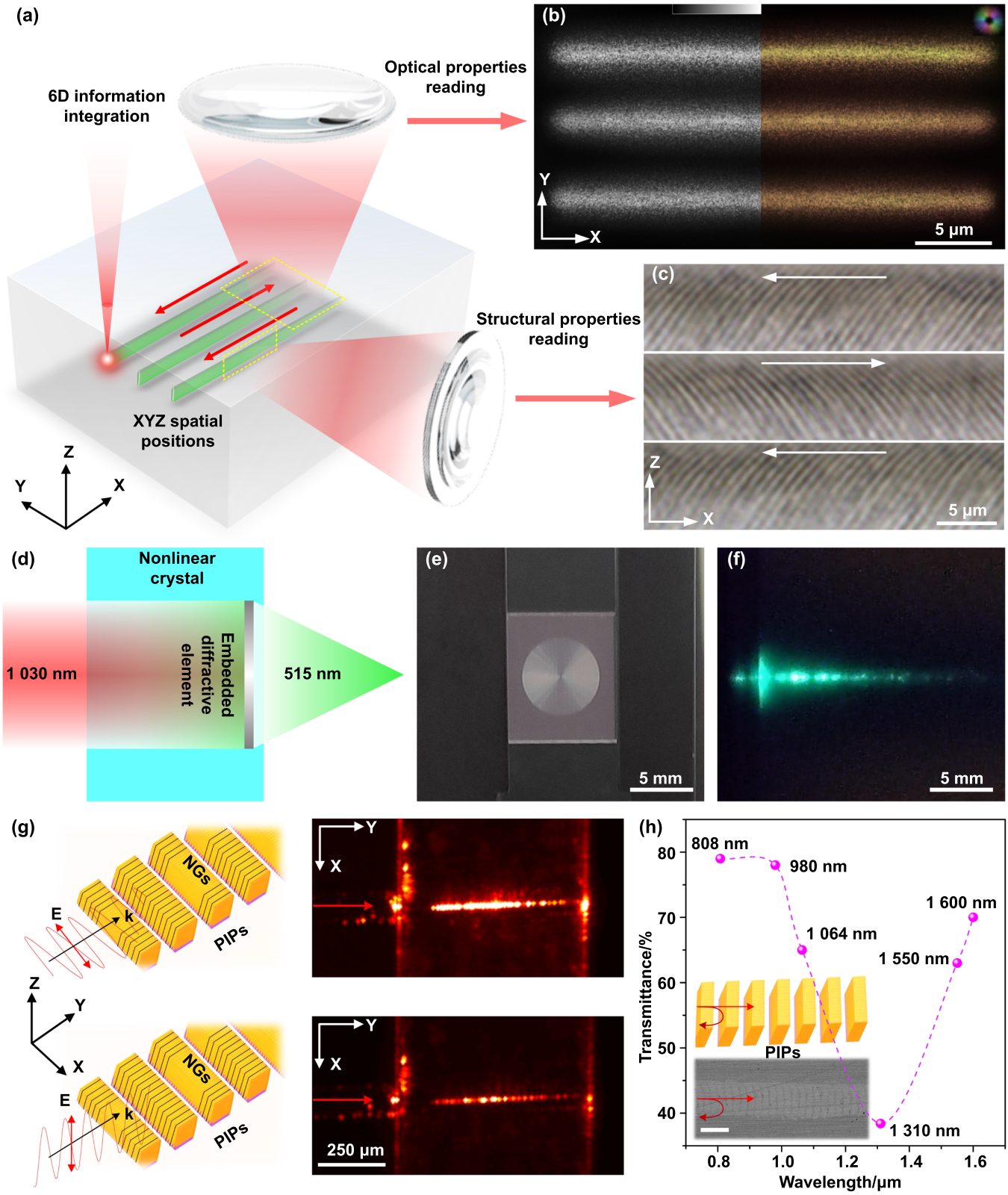

Figure 5. Potential applications of composite structuring. (a) Schematic diagram of multi-dimensional information integration. (b) Optical retardance (left) and azimuth angle (right) of the NGs in fused silica. The color bar illustrates the retardance value (0–250 nm). Pseudocolor indicates the direction of the slow axis. (c) Directional features of the PIPs in fused silica. White arrows indicate the scanning direction. (d) Schematic diagram of the nonlinear diffractive element made of the composite structure. (e) Optical image of a nonlinear planar axicon lens with a diameter of about 6 mm inscribed in lithium niobate crystal. (f) A second harmonic Bessel beam (testing light wavelength: 1 030 nm) was generated by the nonlinear planar axicon lens. (g) Schematic diagram of the polarization selectivity of NGs (left) and corresponding experimental certification (right). E represents the polarization direction. k indicates the wave vector. Probe light wavelength: 980 nm. (h) The wavelength selectivity of PIPs. Insets are schematic diagrams of the selective transmission (upper) and SEM images of PIPs in La_2O_3–Ta_2O_5–Nb_2O_5 glass (lower). Red arrows indicate the incidence of the probe light. Scale bar: 1 μm.

Generally, the laser was focused 10–500 μm below the surface of the sample via a 50 × objective lens (NA = 0.8). For fused silica, the pulse energy is 0.3–2 μJ, the pulse duration is 0.2–4 ps, the repetition rate is 25–200 kHz, and the scanning speed is 10–2000 μm s^{-1}. For unconventional glasses, the pulse energy is 0.5–1.5 μJ, the pulse duration is 0.8–3 ps, the repetition rate is 100–200 kHz, and the scanning speed is 100–2 000 μm s^{-1} (La_2O_3–Nb_2O_5 glass, La_2O_3–ZrO_2–Nb_2O_5 glass, and La_2O_3–Ta_2O_5–Nb_2O_5 glass) and 50–150 μm s^{-1} (La_2O_3–Al_2O_3 glass). For crystals, the pulse energy is 0.5–1 μJ, the pulse duration is 0.5–1 ps, the repetition rate is 50–200 kHz, and the scanning speed is 20–1 600 μm s^{-1}.

4.3. Structural characterization of composite structures

The optical observation of PIPs was performed using a polarizing microscope (BX53 Olympus Ltd). The structural properties of the PIPs and NGs were examined by scanning electron microscopy (SEM), using backscattering mode. For the SEM observation, samples were polished so as to expose the composite structures to air, and the polished surface was etched with hydrofluoric acid to improve the contrast of SEM images. Further phase transition characterization of the crystal-glass heterogeneous interface was performed by focused ion beam slice and transmission electron microscopy.

4.4. Theoretical modelling and simulation

Numerical simulation of the focal light field was performed using a finite-element method mode-solver tool. In the modelling, fused silica is set as the target transparent medium for demonstrating the establishment of the focal-volume interference, and a focused Gaussian beam is set as the original light source. The distance between the light radiation source and the focal plane is determined by the refractive index of the target medium and the numerical aperture of the objective lens.

Data and materials availability

All data needed to evaluate the conclusions in the paper are available in the main text or the supplementary materials.

Acknowledgments

This work was financially supported by the National Key Research and Development Program of China (No. 2021YFB2802001); the National Natural Science Foundation of China (Grant Nos. 12304349, U20A20211, 62275233); the Postdoctoral Fellowship Program of CPSF (GZB20230628, GZC20241465). We wish to thank Nianhang Rong and Xi Zheng of Zhejiang University Analysis Center of Agrobiology and Environmental Sciences for assistance with the SEM examination.

Author contributions

B Z and Z W contributed equally to this work. B Z and Z W conceived the idea. J Q organized, coordinated, and supervised the project. B Z and Z W performed the experiments and collected the data. B Z, Z W, D T and J Q interpreted the results and proposed the structuring mechanism. B Z, Z W and D T wrote the manuscript. M G and Y Y supervised and reviewed the manuscript. B Z, Z W, D T, and J Q discussed and revised the manuscript.

Conflict of interest

The authors declare no competing interests.

ORCID iD

Jianrong Qiu https://orcid.org/0000-0003-3148-2500

References

[1] Zijlstra P, Chon J W M and Gu M 2009 Five-dimensional optical recording mediated by surface plasmons in gold nanorods *Nature* **459** 410–3
[2] Karst J, Floess M, Ubl M, Dingler C, Malacrida C, Steinle T, Ludwigs S, Hentschel M and Giessen H 2021 Electrically switchable metallic polymer nanoantennas *Science* **374** 612–6
[3] Arbabi A, Horie Y, Bagheri M and Faraon A 2015 Dielectric metasurfaces for complete control of phase and polarization with subwavelength spatial resolution and high transmission *Nat. Nanotechnol.* **10** 937–43
[4] Yu N F and Capasso F 2014 Flat optics with designer metasurfaces *Nat. Mater.* **13** 139–50
[5] Hua J Y, Hua E K, Zhou F B, Shi J C, Wang C H, Duan H G, Hu Y Q, Qiao W and Chen L S 2021 Foveated glasses-free 3D display with ultrawide field of view via a large-scale 2D-metagrating complex *Light Sci Appl* **10** 213
[6] Han D D, Zhang Y L, Ma J N, Liu Y Q, Han B and Sun H B 2016 Light-mediated manufacture and manipulation of actuators *Adv. Mater.* **28** 8328–43
[7] Wei D Z *et al* 2018 Experimental demonstration of a three-dimensional lithium niobate nonlinear photonic crystal *Nat. Photonics* **12** 596–600
[8] Zhang Y, Sheng Y, Zhu S N, Xiao M and Krolikowski W 2021 Nonlinear photonic crystals: from 2D to 3D *Optica* **8** 372–81
[9] Chen Y *et al* 2022 Multidimensional nanoscopic chiroptics *Nat. Rev. Phys.* **4** 113–24
[10] Sun L Y *et al* 2019 Separation of valley excitons in a MoS_2 monolayer using a subwavelength asymmetric groove array *Nat. Photonics* **13** 180–4
[11] Li S X, Xia H, Liu T Y, Zhu H, Feng J C, An Y, Zhang X L and Sun H B 2023 In situ encapsulated moiré perovskite for stable photodetectors with ultrahigh polarization sensitivity *Adv. Mater.* **35** 2207771
[12] Lu J F, Tian J, Poumellec B, Garcia-Caurel E, Ossikovski R, Zeng X L and Lancry M 2023 Tailoring chiral optical properties by femtosecond laser direct writing in silica *Light Sci. Appl.* **12** 46
[13] Lu J F, Garcia-Caurel E, Ossikovski R, Courvoisier F, Zeng X L, Poumellec B and Lancry M 2023 Femtosecond laser direct writing multilayer chiral waveplates with minimal linear birefringence *Opt. Lett.* **48** 271–4

[14] Wei D Z *et al* 2019 Efficient nonlinear beam shaping in three-dimensional lithium niobate nonlinear photonic crystals *Nat. Commun.* **10** 4193

[15] Gao J C, Zhao X J, Yan Z, Fu Y H, Qiu J R, Wang L and Zhang J Y 2024 Multi-dimensional shingled optical recording by nanostructuring in glass *Adv. Funct. Mater.* **34** 2306870

[16] Ouyang X *et al* 2021 Synthetic helical dichroism for six-dimensional optical orbital angular momentum multiplexing *Nat. Photon.* **15** 901–7

[17] Zhang B, Tan D Z, Wang Z, Liu X F, Xu B B, Gu M, Tong L M and Qiu J R 2021 Self-organized phase-transition lithography for all-inorganic photonic textures *Light Sci. Appl.* **10** 93

[18] Papadopoulos A, Skoulas E, Mimidis A, Perrakis G, Kenanakis G, Tsibidis G D and Stratakis E 2019 Biomimetic omnidirectional antireflective glass via direct ultrafast laser nanostructuring *Adv. Mater.* **31** 1901123

[19] Zhang B, Wang Z, Tan D Z and Qiu J R 2023 Ultrafast laser-induced self-organized nanostructuring in transparent dielectrics: fundamentals and applications *PhotoniX* **4** 24

[20] Wang Z, Zhang B, Wang Z Q, Zhang J, Kazansky P G, Tan D Z and Qiu J R 2023 3D imprinting of voxel-level structural colors in lithium niobate crystal *Adv. Mater.* **35** 2303256

[21] Djogo G, Li J Z, Ho S, Haque M, Ertorer E, Liu J, Song X L, Suo J and Herman P R 2019 Femtosecond laser additive and subtractive micro-processing: enabling a high-channel-density silica interposer for multicore fibre to silicon-photonic packaging *Int. J. Extrem. Manuf.* **1** 045002

[22] Lu Y, Kai L, Chen C Y, Yang Q, Meng Y Z, Liu Y, Cheng Y, Hou X and Chen F 2022 Nanochannels with a 18-nm feature size and ultrahigh aspect ratio on silica through surface assisting material ejection *Adv. Photon. Nexus* **1** 026004

[23] Hecker S, Blothe M and Graf T 2020 Reproducible process regimes during glass welding by bursts of subpicosecond laser pulses *Appl. Opt.* **59** 11382–8

[24] Hecker S, Blothe M, Grossmann D and Graf T 2020 Process regimes during welding of glass by femtosecond laser pulse bursts *Appl. Opt.* **59** 6452–8

[25] Ródenas A, Gu M, Corrielli G, Paiè P, John S, Kar A K and Osellame R 2019 Three-dimensional femtosecond laser nanolithography of crystals *Nat. Photonics* **13** 105–9

[26] Jia Y C, Wang S X and Chen F 2020 Femtosecond laser direct writing of flexibly configured waveguide geometries in optical crystals: fabrication and application *Opto-Electron. Adv.* **3** 190042

[27] Jin F, Liu J, Zhao Y Y, Dong X Z, Zheng M L and Duan X M 2022 λ/30 inorganic features achieved by multi-photon 3D lithography *Nat. Commun.* **13** 1357

[28] Zhang X L, Yu F, Chen Z G, Tian Z N, Chen Q D, Sun H B and Ma G C 2022 Non-Abelian braiding on photonic chips *Nat. Photon.* **16** 390–5

[29] Sugioka K 2019 Hybrid femtosecond laser three-dimensional micro-and nanoprocessing: a review *Int. J. Extrem. Manuf.* **1** 012003

[30] Von der Linde D, Sokolowski-Tinten K and Bialkowski J 1997 Laser–solid interaction in the femtosecond time regime *Appl. Surf. Sci.* **109–110** 1–10

[31] Stuart B C, Feit M D, Herman S, Rubenchik A M, Shore B W and Perry M D 1996 Nanosecond-to-femtosecond laser-induced breakdown in dielectrics *Phys. Rev.* B **53** 1749–61

[32] Du D, Liu X, Korn G, Squier J and Mourou G 1994 Laser-induced breakdown by impact ionization in SiO_2 with pulse widths from 7 ns to 150 fs *Appl. Phys. Lett.* **64** 3071–3

[33] Tsibidis G D and Stratakis E 2020 Ionisation processes and laser induced periodic surface structures in dielectrics with mid-infrared femtosecond laser pulses *Sci. Rep.* **10** 8675

[34] Schaffer C B, Brodeur A and Mazur E 2001 Laser-induced breakdown and damage in bulk transparent materials induced by tightly focused femtosecond laser pulses *Meas. Sci. Technol.* **12** 1784–94

[35] Itoh K, Watanabe W, Nolte S and Schaffer C B 2006 Ultrafast processes for bulk modification of transparent materials *MRS Bull.* **31** 620–5

[36] Taylor R, Hnatovsky C and Simova E 2008 Applications of femtosecond laser induced self-organized planar nanocracks inside fused silica glass *Laser Photonics Rev.* **2** 26–46

[37] Rajeev P P, Gertsvolf M, Hnatovsky C, Simova E, Taylor R S, Corkum P B, Rayner D M and Bhardwaj V R 2007 Transient nanoplasmonics inside dielectrics *J. Phys. B: At. Mol. Opt. Phys.* **40** S273–82

[38] Bhardwaj V R, Simova E, Rajeev P P, Hnatovsky C, Taylor R S, Rayner D M and Corkum P B 2006 Optically produced arrays of planar nanostructures inside fused silica *Phys. Rev. Lett.* **96** 057404

[39] Hnatovsky C, Taylor R S, Rajeev P P, Simova E, Bhardwaj V R, Rayner D M and Corkum P B 2005 Pulse duration dependence of femtosecond-laser-fabricated nanogratings in fused silica *Appl. Phys. Lett.* **87** 014104

[40] Shimotsuma Y, Kazansky P G, Qiu J R and Hirao K 2003 Self-organized nanogratings in glass irradiated by ultrashort light pulses *Phys. Rev. Lett.* **91** 247405

[41] Zhang F T, Nie Z G, Huang H X, Ma L, Tang H, Hao M M and Qiu J R 2019 Self-assembled three-dimensional periodic micro-nano structures in bulk quartz crystal induced by femtosecond laser pulses *Opt. Express* **27** 6442–50

[42] Yang W J, Bricchi E, Kazansky P G, Bovatsek J and Arai A Y 2006 Self-assembled periodic sub-wavelength structures by femtosecond laser direct writing *Opt. Express* **14** 10117–24

[43] Lu J F, Dai Y, Li Q, Zhang Y L, Wang C H, Pang F F, Wang T Y and Zeng X L 2019 Fiber nanogratings induced by femtosecond pulse laser direct writing for in-line polarizer *Nanoscale* **11** 908–14

[44] Cao J, Mazerolles L, Lancry M, Brisset F and Poumellec B 2017 Modifications in lithium niobium silicate glass by femtosecond laser direct writing: morphology, crystallization, and nanostructure *J. Opt. Soc. Am.* B **34** 160–8

[45] Zhang J Y, Gecevičius M, Beresna M and Kazansky P G 2014 Seemingly unlimited lifetime data storage in nanostructured glass *Phys. Rev. Lett.* **112** 033901

[46] Shimotsuma Y, Sakakura M, Kazansky P G, Beresna M, Qiu J R, Miura K and Hirao K 2010 Ultrafast manipulation of self-assembled form birefringence in glass *Adv. Mater.* **22** 4039–43

[47] Wang Y T, Lancry M, Cavillon M and Poumellec B 2022 Lifetime prediction of nanogratings inscribed by a femtosecond laser in silica glass *Opt. Lett.* **47** 1242–5

[48] Wang Z, Zhang B, Tan D Z and Qiu J R 2023 Ostensibly perpetual optical data storage in glass with ultra-high stability and tailored photoluminescence *Opto-Electron. Adv.* **6** 220008

[49] Wang M H *et al* 2021 Femtosecond laser fabrication of nanograting-based distributed fiber sensors for extreme environmental applications *Int. J. Extrem. Manuf.* **3** 025401

[50] Eaton S M, Zhang H B, Herman P R, Yoshino F, Shah L, Bovatsek J and Arai A Y 2005 Heat accumulation effects in femtosecond laser-written waveguides with variable repetition rate *Opt. Express* **13** 4708–16

[51] Kawata S, Sun H B, Tanaka T and Takada K 2001 Finer features for functional microdevices *Nature* **412** 697–8

[52] Tan D Z, Zhang B and Qiu J R 2021 Ultrafast laser direct writing in glass: thermal accumulation engineering and applications. *Laser Photon. Rev.* **15** 2000455